Journal of Catalysis 264 (2009) 77–87

Contents lists available at ScienceDirect

Journal of Catalysis

journal homepage: www.elsevier.com/locate/jcat

Product shape selectivity dominates the Methanol-to-Olefins (MTO) reaction over H-SAPO-34 catalysts

Bart P.C. Hereijgers [a,c], Francesca Bleken [a], Merete H. Nilsen [a], Stian Svelle [a], Karl-Petter Lillerud [a], Morten Bjørgen [b], Bert M. Weckhuysen [c], Unni Olsbye [a,*]

[a] inGAP Center of Research-Based Innovation, Department of Chemistry, University of Oslo, Sem Sælands vei 26, N-0315 Oslo, Norway
[b] Department of Chemistry, Norwegian University of Science and Technology, N-7491 Trondheim, Norway
[c] Inorganic Chemistry and Catalysis, Debye Institute for NanoMaterials Science, Utrecht University, 3584 CA Utrecht, The Netherlands

ARTICLE INFO

Article history:
Received 26 January 2009
Accepted 5 March 2009
Available online 25 April 2009

Keywords:
Methanol-to-hydrocarbons
MTH
Shape selectivity
Deactivation
Methanol
Zeolite
Zeotype

ABSTRACT

Selectivity control is a major issue in chemical processes. In this work, isotopic switch experiments ($^{12}CH_3OH//^{13}CH_3OH$) were used to study the relationship between reaction intermediates and product distribution for the Methanol-to-Olefins (MTO) reaction over the archetype H-SAPO-34 catalyst during a full deactivation cycle. After switching, all alkenes contained a major fraction of ^{13}C, and this fraction was only slightly influenced by catalyst deactivation. Among the methylbenzene intermediates, the ^{13}C fraction decreased with a decreasing number of methyl groups on the aromatic ring, throughout the test cycle. These observations clearly demonstrate that an observed increase in ethene selectivity with time on stream is due to product shape selectivity, which changes with the degree of pore clogging. Quantification of labeled and unlabeled methylbenzenes showed that less than 10% of the catalyst cages contained an active methylbenzene intermediate at any time during the test, even for 1 μm crystal size.

1. Introduction

The methanol-to-hydrocarbons (MTH) reaction constitutes the final step in the upgrading of natural gas, coal, or biomass to fuels and petrochemical products [1]. The reaction is carried out over protonated zeolite or zeotype materials, and is generally observed to proceed by conversion of methanol into dimethyl ether (DME) and water, followed by a kinetic induction period leading to formation of hydrocarbons (and more water). If space permits, alkene formation is followed by co-production of aromatics and alkanes [2]. Although more than 20 different mechanisms have been proposed for the MTH reaction [3], there is now general consensus about the so-called "hydrocarbon pool" mechanism, initially proposed by Dahl and Kolboe, in which methyl groups are constantly added to the pool by reaction with methanol, and alkenes are subsequently split off [4–6]. Independent research by several groups points to multiply methylated benzene molecules, hereinafter called polymethylbenzenes (polyMBs), as main intermediates in the MTH reaction [7–23]. The active site in MTH catalysts is thus not the Brönsted acid site alone, but an organic–inorganic hybrid material consisting of a proton in close interaction with a polyMB molecule. Alkenes may be produced by formation of a polymethylbenzenium ion, which splits off alkenes by ring contraction followed by hydride or methyl transfer. This is followed by rearrangement and deprotonation to a benzene ring with fewer methyl groups. This reaction is called the paring reaction (Supplementary material, Scheme 1) [18,23,24]. An alternative route to the formation of alkenes, originally proposed by Mole et al. and further elaborated by Haw et al., is the so-called exocyclic methylation reaction. In this reaction scheme, a methyl group in the polymethylbenzenium ion is deprotonated, leading to formation of an exocyclic double bond which is subsequently methylated and split off as an alkene molecule (Supplementary material, Scheme 2) [25,26].

Product shape selectivity and transition-state shape selectivity have been reported for the MTH reaction. Evidence of product shape selectivity is found, e.g. in the work of Haw and co-workers [26], where the MFI structure of H-ZSM-5 (i.e., a three-dimensional 10-ring structure with 5.1 × 5.5 and 5.3 × 5.6 Å window dimensions) is shown to produce a mixture of alkenes, alkanes and a major fraction of aromatics up to durene (1,2,4,5-tetramethylbenzene), when tested at 450 °C [26]. Under the same test conditions, the CHA structure of H-SAPO-34 (i.e., a three-dimensional cage structure with 3.8 × 3.8 Å window dimensions) produces mainly C_2–C_4 alkenes [26]. Auroux et al. [27] have compared the performances of the MFI structure to those of the AFI structure of

* Corresponding author. Fax: +47 22 85 54 41.
E-mail address: unni.olsbye@kjemi.uio.no (U. Olsbye).

0021-9517/$ - see front matter © 2009 Elsevier Inc. All rights reserved.
doi:10.1016/j.jcat.2009.03.009

H-SSZ-24 (i.e., a one-dimensional 12-ring structure with 7.3 × 7.3 Å window dimensions) at 370 °C. While the products observed over the MFI structure are the same as quoted above, the larger pore diameter of the AFI structure allows for the production of aromatics, including penta- and hexamethylbenzene, and naphthalene [27]. As a result, a correlation can be made between the dimensions of the largest main product and the window dimensions of these three molecular sieve structures.

Transition-state shape selectivity in the MTH reaction was recently demonstrated by comparing the product selectivity of 10-ring H-ZSM-5 and 12-ring H-Beta zeolite, respectively, while studying the main reaction intermediates of the two topologies during ^{12}C-/^{13}C-methanol transient experiments. More specifically, in H-Beta zeolite, hexamethylbenzene (hexaMB) was found to be the major reaction intermediate, favoring formation of propene and butenes [18,28]. On the other hand, in H-ZSM-5, the active hydrocarbon pool was observed to be sterically restricted to methylbenzenes with 1–3 methyl groups, favoring the formation of ethene and propene [28,30]. Thorough investigation of the isotopic distribution in the gas phase products formed over H-ZSM-5 revealed that olefin methylation and cracking reactions constitute an important, additional route to C_3^+ alkene formation, while ethene is formed predominantly from aromatic intermediates [29,30].

The archetype Methanol-to-Olefins (MTO) catalyst, namely H-SAPO-34, is composed of double 6-rings that are stacked in an ABC pattern. This stacking leads to a 3-dimensional 8-ring channel structure with cages at channel intersections. The opening of the cage windows is 3.8 × 3.8 Å and the dimension of the cage is 7.3 Å × 12 Å [1]. By catalytic testing and isotopic labeling experiments, we will demonstrate that product distribution in H-SAPO-34 is governed by product shape selectivity only, even for severely coked catalysts. This conclusion closes a decade-long debate on the selectivity issue for the MTO reaction over H-SAPO-34, where both transition-state shape selectivity and product shape selectivity have been argued for [31,34].

For example, Chen et al. have studied the influence of crystal size in H-SAPO-34 catalysts for the MTO reaction at 425 °C with crystal sizes ranging from 0.25 μm to 2.5 μm [31]. They reported that the initial product distribution was independent of crystal size and, furthermore, that increasing coke contents led to an increasing ethene-to-propene ratio. A correlation between ethene-to-propene ratio and pore volume was observed for the coked samples, with no effect of crystal size. Based on these results, Chen et al. concluded that product distribution in H-SAPO-34 is governed by transition-state shape selectivity [31]. Interestingly, in a parallel publication, Dahl et al. studied the conversion of propanol and ethanol over the same catalyst batches as those used by Chen et al., but reached different conclusions [32]. More specifically, Dahl et al. observed that propanol, which rapidly dehydrates to propene, reacted with an effectiveness factor of 0.96 over the smallest crystals (0.25 μm), while the effectiveness factor decreased to 0.87 and 0.36 over medium-sized (0.5 μm) and large-sized (2.5 μm) crystals, respectively, at 400 °C. On the other hand, ethene (i.e., dehydrated ethanol) conversion was not diffusion limited in any of the crystals at 400 °C. Based on these results, Dahl et al. concluded that the increasing ethene-to-propene ratios observed during the MTO reaction over H-SAPO-34 with time on stream is due to increasing diffusion barriers introduced by coke formation [32].

Later, Haw and co-workers performed a systematic study of effluent product composition and retained hydrocarbons during the MTO reaction over H-SAPO-34 catalyst at 400 °C by using GC analysis and solid-state MAS ^{13}C NMR, respectively. A methanol flow was first fed over the catalyst, then replaced by a He flow at the reaction temperature for a predetermined time, followed by thermal quenching. An increasing ethene-to-propene ratio in the effluent was observed with increasing flush duration. Concurrently, a decrease in the ratio of methyl versus aromatic carbon atoms in the catalyst was observed by NMR, and the authors ascribed this decrease to a decreasing number of methyl groups in the polymethylbenzene intermediates, due to alkene formation in the absence of methanol. The apparent inverse correlation between ethene-to-propene ratio and number of methyl groups on the polyMB intermediates led to the conclusion that product selectivity in H-SAPO-34 is governed by transition-state shape selectivity [33]. Inspired by these results, Song and Haw elegantly modified the cage size of H-SAPO-34 in a later study, by introducing phosphate groups into the structure through ship-in-a-bottle synthesis from PH_3 [35]. Lower methanol conversions and higher ethene selectivities were reported for the phosphate-modified samples compared to the mother sample [35].

Finally, Barger measured the ethene-to-propene ratio in the effluent of an MTO reactor when testing H-SAPO-34 catalysts at various temperatures, and made a plot of this ratio versus the ethene-to-propene ratio expected from thermodynamic equilibrium in gas phase at the same temperatures. A linear correlation was observed, and Barger concluded that product distribution over H-SAPO-34 is governed by product shape selectivity [34].

The transient isotopic labeling experiments performed in this study led to improved understanding of the deactivation mechanism in H-SAPO-34 catalysts. It is well known that the intermediate polyMBs in H-SAPO-34 are gradually converted to less active polycyclic aromatic molecules with time on stream [11,36,37]. In the present contribution, we observed that there is no straightforward correlation between the formation of polycyclic aromatics and catalyst deactivation. Instead, polycyclic aromatics are shown to be formed predominantly from methanol and product molecules, which are trapped inside deactivated catalyst crystals. Moreover, the results presented in this study confirm the conclusions of Dahl [32] and Barger [34], pointing toward the importance of product shape selectivity for controlling the product distribution over H-SAPO-34 molecular sieves.

2. Materials and methods

2.1. Catalyst synthesis

Small crystals of SAPO-34 were synthesised by modifying Example 35 mentioned in Ref. [38]. The molar composition of the gel was P_2O_5:Al_2O_3:0.1 SiO_2:0.4 TEAOH:15.7 H_2O. Ortho-phosphoric acid (15.4 g, 85%, Merck) and water (38.7 g) were mixed, before the addition of aluminum isopropoxide (27.2 g, Aldrich) and Ludox LS-40 (4.0 g, Sigma–Aldrich). The mixture was stirred for 10 min between each addition. The structure-directing agent, tetraethylammonium hydroxide (TEAOH, 49.2 g, 35%, Aldrich) was added, and the resulting gel was stirred at room temperature for 24 h, thereafter transferred to a Teflon liner and heated under tumbling at 200 °C for 3 days.

Larger crystals of SAPO-34 were obtained by using morpholine as the structure-directing agent, as described by Ito et al. [39]. The molar composition of the gel was P_2O_5:1.2 Al_2O_3:0.4 SiO_2:0.6 morpholine: 38.5 H_2O. Ortho-phosphoric acid (1.6 g, 85%) and water (18.02 g), AlOOH (1.0 g, Condea Vista Company) and colloidal silica (Ludox LS-40) were mixed, the solution was stirred for 10 min between each addition. Morpholine (1.5 g, 98%, Fluka) was added, and the resulting gel was stirred for 1 h. Crystallization was carried out at static conditions at 200 °C for 3 days.

The resulting crystals were washed with distilled water, centrifugated, and dried overnight at 100 °C. The H-SAPO-34 form was obtained by calcination in air at 550 °C for 6 h. In the following, the samples are referred to as H-SAPO-34 (1 μm) and H-SAPO-34 (5 μm).

2.2. Catalyst characterization

The phase and crystallinity of the samples were characterized by X-ray powder diffraction (XRD) on a Siemens Bruker D5000 with monochromatic Cu $K\alpha_1$-radiation. The morphology and particle size were determined using scanning electron microscope (SEM). SEM was performed on a FEI Quanta 200 FEG-ESEM. The samples were placed on a carbon film, and no coating of the samples was used. Elemental composition was measured by inductively coupled plasma atomic absorption spectroscopy (ICP-AES) using a Varian Vista AX CCD axial ICP-AES. Transmission FTIR spectra of self-supporting sample wafers were recorded at 2 cm^{-1} resolution by a BioRad FTS 80 spectrometer, equipped with a liquid N_2 cooled MCT (mercury–cadmium–telluride) detector. The wafers were mounted in a quartz cell with NaCl windows designed for adsorption measurements at −196 °C. The samples were pre-treated for 1 h at 450 °C in vacuum and subsequently cooled before CO was admitted to the cell at −196 °C.

2.3. Catalyst testing

Catalyst testing was performed in a fixed bed glass reactor at 350 °C over 60 mg catalyst with particle size 250–420 μm. $WHSV_{MeOH}$ was 6.2 h^{-1} obtained by flowing He gas (28 mL/min) through a methanol saturator at 20 °C (P(MeOH) = 140 hPa). ^{12}C-methanol was obtained from VWR (99.8% purity), while ^{13}C-methanol was obtained from ICON (99% ^{13}C). Analysis of the product stream was performed with a gas chromatograph (GC) (Agilent 6890) equipped with HP-PONA column and FID detector parallel to an HP-PoraPLOT Q column in series with a HP-5 molsieve column and TC detector. On-line mass spectrometry was performed with a Pfeiffer Vacuum OmniStar mass spectrometer. Fragments with m/z = 31 (methanol), m/z = 46 (DME), and m/z = 4 (He) were followed to monitor the conversion. After a predetermined time on stream, the catalyst was thermally quenched. Off-line analysis of the effluent gas in flushing and isotopic switch experiments (see below) was performed with a HP 6890 gas chromatograph equipped with a GS-GASPRO column and a HP 5973 mass selective detector.

Flushing experiments, in which the methanol-containing feed was replaced by a pure He feed, were performed by switching 4-way valves at the entrance and exit of the methanol saturator, respectively, in order for the He flow to bypass the saturator.

Transient isotopic labeling experiments were performed by using two parallel feed lines, one in which He was led through a saturator containing ^{12}C-methanol, and another in which He was led through a saturator containing ^{13}C-methanol, and rapidly switching between them.

Hydrocarbons that were retained in the catalyst after testing were investigated by dissolution experiments. Typically, 15 mg of the spent catalyst was dissolved in 1 mL 15% HF in a Teflon container. The organic compounds were extracted from the water phase by the addition of 1 mL CH_2Cl_2 containing C_2Cl_6 as internal standard. Analysis of the extracted phase was performed on an Agilent 6890 GC system equipped with either a HP-5MS or a HP-Innovax column and an Agilent 5973 Network Mass Selective Detector. Hereinafter, the term "Retained hydrocarbons" is used to describe all compounds that are detectable by this method.

The total amount of oxidizable material in the catalyst after testing, hereinafter called "Coke", was analyzed by thermogravimetric analysis (TGA). Typically, 8–12 mg of the spent catalyst was heated in a pure oxygen flow with 5 °C/min heating rate to 550 °C and was held isothermal for 1 h.

3. Results

3.1. Catalyst characterization

SEM micrographs of the two H-SAPO-34 catalyst materials under study are shown in Fig. 1, while X-ray diffractograms are shown in Supplementary material, Figure S1.

The XRD and SEM results show that well-crystallined H-SAPO-34 of different particle sizes has been obtained. The SEM pictures (Fig. 1) show that the smaller crystals are 1 μm, and the larger 5 μm, in average diameter. Both catalysts are well defined both in crystal shape and in size. The (Al + P)/Si-ratios, as determined by ICP-AES, are 10 and 3 for H-SAPO-34 (1 μm) and H-SAPO-34 (5 μm), respectively. The (Al + P)/Si-ratio of H-SAPO-34 (1 μm) corresponds to one silicon atom per cage, i.e., one Brönsted site per cage. For H-SAPO-34 (5 μm), which is synthesised using morpholine as template, the (Al + P)/Si-ratio is lower, due to the need of two protons to balance the charge of two morpholine molecules per cage [40]. The acidic properties of both samples were assessed by FTIR using CO as molecular probe (see Supplementary material, Figures S2 and S3). The Brönsted sites of both samples showed equal shifts in the ν(OH) frequency when CO was adsorbed. Also the ν(CO) frequencies were equally shifted upon adsorption on the two samples, thus confirming virtually identical acid strengths. Lewis acidity was not detected for any of the samples, but H-SAPO-34 (5 μm) has a significant concentration of Si–OH sites, both on the external surface of the crystallites and in internal defects. Consequently, a part of Si present in this sample will not give rise to

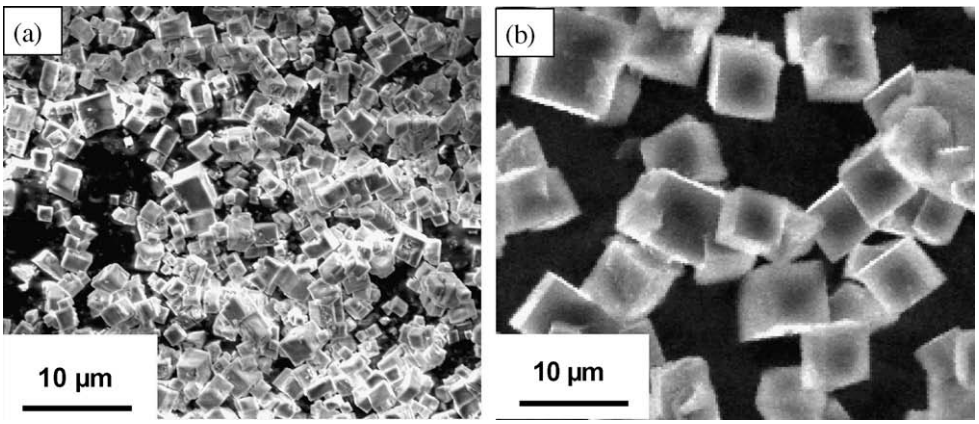

Fig. 1. SEM pictures of the two catalyst batches. (a) H-SAPO-34 (1 μm) and (b) H-SAPO-34 (5 μm).

Brönsted acidity. A minor component representing amorphous Al species was also observed for H-SAPO-34 (5 μm).

3.2. MTO reaction studies

Methanol conversion and product selectivity data, as well as the total amount of coke deposits in the catalysts after various times on stream at 350 °C, are shown in Fig. 2. Both catalysts have a short induction period, reaching close to full conversion after approximately 3 min on stream (observed by mass spectrometry analysis of the effluent, see Supplementary material). The smallest catalyst crystals (H-SAPO-34 (1 μm)) are active for almost 100 min on stream before losing >95% of their activity, while the larger size crystals (H-SAPO-34 (5 μm)) lose 95% of their activity after only 15 min on stream (Fig. 2a and c). The observed influence of H-SAPO-34 crystal size and Si site density on catalyst deactivation is in accordance with the previous reports [41,42]. Important differences in product selectivity are observed for H-SAPO-34 (1 μm) compared to H-SAPO-34 (5 μm): The initial propene selectivity is significantly higher for H-SAPO-34 (1 μm) (40% vs. 30%, respectively), while the initial ethene selectivity is correspondingly higher for H-SAPO-34 (5 μm) (30% vs. 22%, respectively), and is comparable to the propene selectivity for this catalyst. The initial C_4 selectivity is ~20% for both catalysts. Further, H-SAPO-34 (5 μm) has initially significantly higher propane selectivity than H-SAPO-34 (1 μm) (16% vs. 5%) (Fig. 2b and d). This result indicates that intermolecular hydride transfer reactions, leading to the formation of aromatics and alkanes, are more important in the larger crystals after short times on stream.

The total amount of oxidizable material ("coke") in the catalyst is also observed to depend on crystal size and Si content: A more rapid increase in the coke content is observed by thermogravimetric analysis for the larger crystals compared to the smaller crystals (Fig. 2a and c), in line with the alkane selectivity in the gas phase (see above). It is interesting to note that the total coke content is not too different between the two catalysts after complete deactivation: In H-SAPO-34 (1 μm) it amounts to 16.5 wt%, while in H-SAPO-34 (5 μm) it amounts to 14.0 wt%.

The composition of retained hydrocarbons in each catalyst after various times on stream is shown in Figs. 3 and 4. Fig. 3 shows the time dependence for H-SAPO-34 (1 μm). Initially, the retained hydrocarbons consist mainly of methylbenzenes (MBs), with tetramethylbenzenes (tetraMBs) as the main constituent. With time on stream, lighter methylbenzenes, as well as heavier bi- and poly-cyclic aromatic molecules, increase in abundance, while tetraMBs decrease. After 80 min on stream, when the catalyst is already heavily deactivated, the residue contains small amounts of phenanthrenes and pyrenes. A similar trend in the development of retained aromatic compounds in H-SAPO-34 with time on stream has been reported previously [11,43]. However, while these previous studies followed the residues only during the active period of the catalyst, we extended the study beyond this point. It can be deduced from Fig. 3 that when extending the period of methanol feed beyond the period where significant

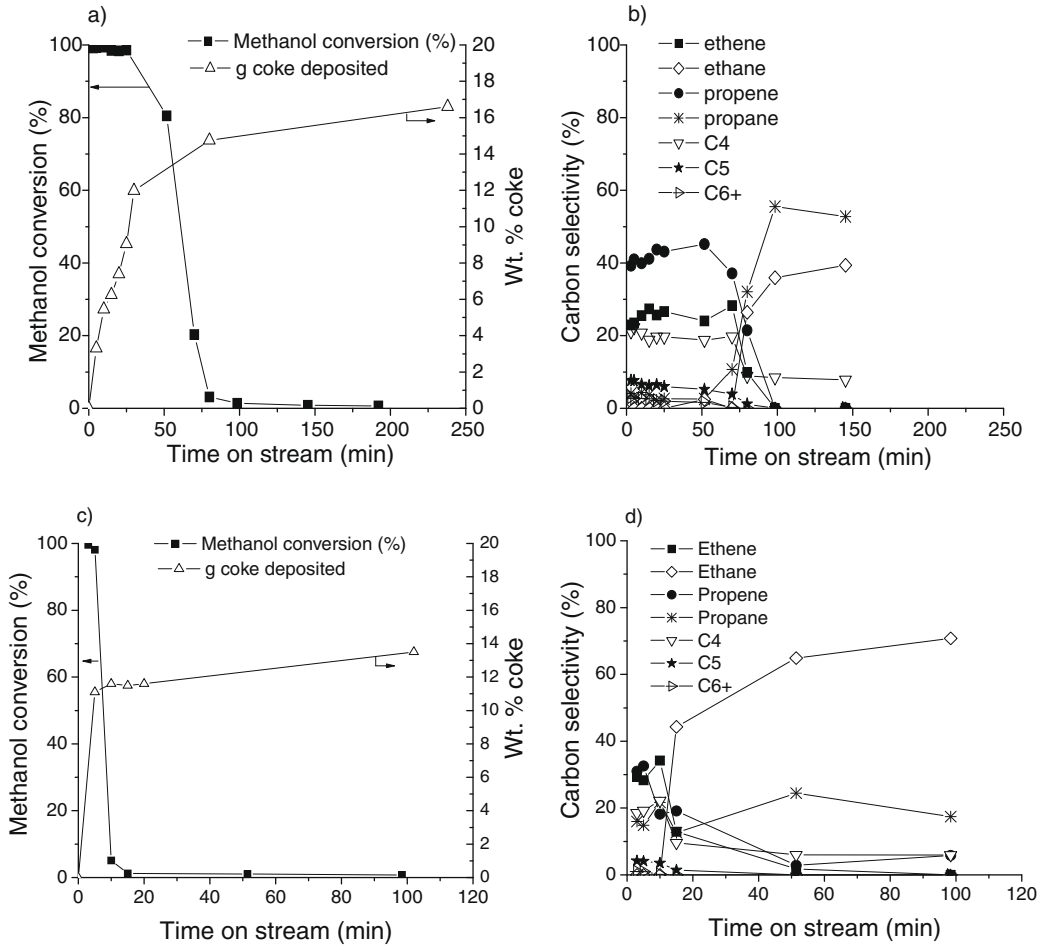

Fig. 2. Methanol conversion and total "coke" content based on thermogravimetric oxidation (a and c) and product selectivity (b and d) obtained over catalysts H-SAPO-34 (1 μm) (a and b) and H-SAPO-34 (5 μm) (c and d) at 350 °C, WHSV = 6.2 g/gh and P(MeOH) = 140 hPa.

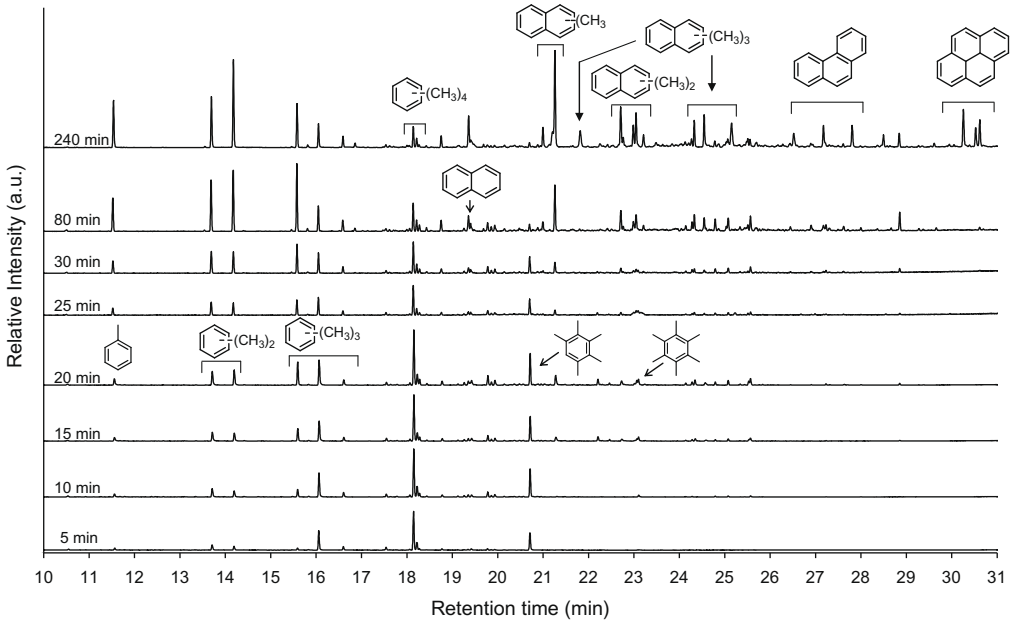

Fig. 3. Gas chromatograms showing the composition of the retained hydrocarbons in H-SAPO-34 (1 μm) catalyst after various times on stream at 350 °C, WHSV = 6.2 g/gh and P(MeOH) = 140 hPa.

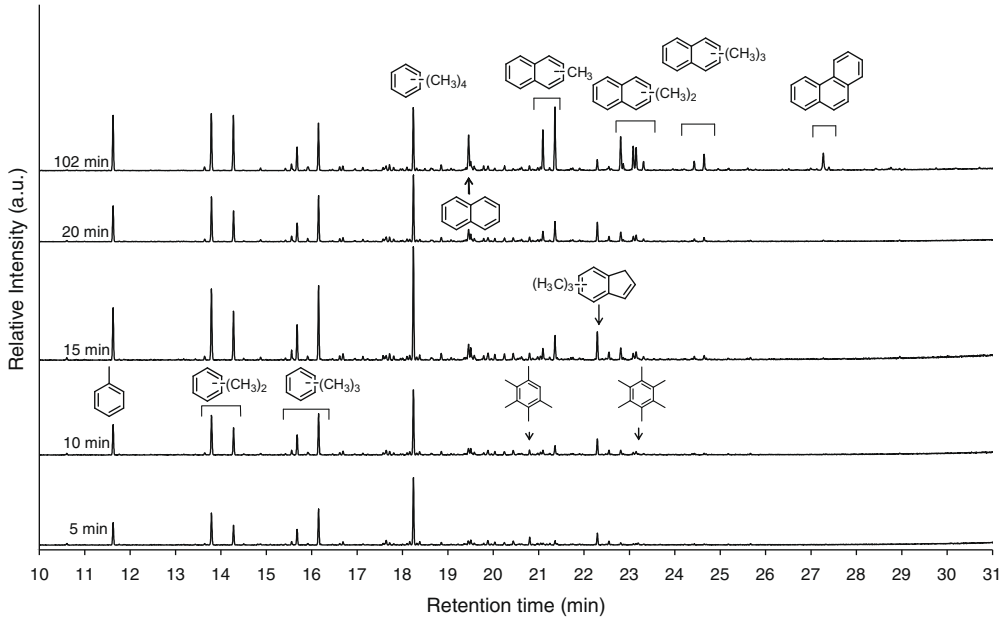

Fig. 4. Gas chromatograms showing the composition of the retained hydrocarbons in H-SAPO-34 (5 μm) catalyst after various times on stream at 350 °C, WHSV = 6.2 g/gh and P(MeOH) = 140 hPa.

methanol conversion takes place (i.e.; >80 min on stream, see Fig. 2a), the retained hydrocarbons continue to increase in abundance, and are further shifted toward the heavier constituents. This result could signify either that the catalytic sites are still accessible to methanol after the catalyst has lost most of its activity, or that the continued formation of aromatic molecules during this period is due to reactions of light, not detectable, molecules that are trapped inside inactive catalyst crystals, or both.

Fig. 4 shows the evolution of retained hydrocarbons in H-SAPO-34 (5 μm) with increasing time on stream. As for H-SAPO-34 (1 μm), the residue consists initially of methylbenzenes, with tetraMBs as the most abundant compound, and the composition of the residue is shifted toward lighter methylbenzenes and bi- and polycyclic aromatic molecules with time on stream. Compared to H-SAPO-34 (1 μm), it is interesting to note that at the time of near complete deactivation (15 min on stream, compare Figs. 2b and 4), H-SAPO-34 (5 μm) contains only small amounts of indenes and methylnaphthalenes, but no traces of the polycyclic aromatic molecules which were observed for H-SAPO-34 (1 μm) at the time of near complete deactivation (80 min on stream, compare Figs. 2a and 3). Again, when feeding methanol beyond the time of near complete deactivation, the amount of hydrocarbon residues increases and is shifted toward heavier compounds.

The amount of retained hydrocarbons in each catalyst (restricted to the methylbenzenes) at different times on stream, in moles per H-SAPO-34 cage as well as in wt% of the catalyst, is

shown in Supplementary material, Figures S4–S6. After 5 min on stream, the molar amount of methylbenzenes corresponds to one MB molecule for every 10H-SAPO-34 cage, in both catalysts. The maximum amount of MBs in either catalyst is less than 25% of the number of H-SAPO-34 cages throughout the active period of the catalyst (i.e., 100 min on stream for the smaller, and 15 minutes on stream for the larger, H-SAPO-34 crystals). A comparison between the amount of retained hydrocarbons and the amount of coke reveals that the amount of coke (in wt% of the catalyst) is 3–6 times higher than the amount of retained methylbenzenes at all times on stream, even initially when no insoluble coke was observed during the dissolution-extraction procedure. The difference is particularly large for the larger crystals, for which the coke content increases very rapidly during the first 5 min on stream. This observation could suggest that a large fraction of the coke is in fact smaller molecules that are not detectable by the dissolution-extraction method, but are nevertheless trapped inside the catalyst crystals.

A comparison between the retained hydrocarbons in the two catalysts reveals that its composition is not the same at the time of near complete deactivation in the two catalysts (compare Figs. 3 and 4). This result may suggest that there is no straightforward correlation between the composition of the retained hydrocarbons and the observed loss of catalyst activity.

3.3. Flushing experiments

The H-SAPO-34 samples were subjected to further studies by flushing the catalysts with He after feeding methanol to full activity, i.e., 3 min on stream (See Supplementary material, Figure S7). The effluent composition and retained hydrocarbons were monitored by MS, GC and dissolution-extraction experiments. GC analysis (see Supplementary material, Figure S8) showed that C_2–C_4 alkene production continued during the first minute of flushing, but decreased to close to zero production after 5 min of flushing, over both catalysts. No obvious trend in product selectivity with flushing time was observed for either catalyst. The amount and composition of aromatic molecules retained in the catalysts after 0–5 min of flushing is shown in Fig. 5 a and b for H-SAPO-34 (1 μm) and H-SAPO-34 (5 μm), respectively. The evolution of retained hydrocarbons with flushing time is similar for the two catalysts: During the first minute, the amount of all aromatic molecules from toluene to pentaMB increases, while the amount of hexaMB decreases to zero. From 1 to 2 min of flushing, all lower methylbenzenes (less than 5 methyl groups) continue to grow, while the amount of pentaMB decreases. The observed decrease in the amount of penta- and hexaMB is in agreement with the previous studies [44], and suggests that these higher polyMBs are converted to alkenes and lower methylbenzenes as outlined in Supplementary material, Schemes 1 and 2. However, it is interesting to note that the amount of lower methylbenzenes formed during flushing far exceeds the penta- and hexaMB consumption, leading to a significant increase in the total amount of aromatic molecules in the catalyst: While the total amount of methylbenzenes (MBs) at the start of the flushing period is 0.03 MB molecules per H-SAPO-34 cage in the smaller crystals (Fig. 5a) and 0.05 MB molecules per H-SAPO-34 cage in the larger crystals (Fig. 5b), it increases by a factor of approximately two in both the smaller and the larger crystals, during the first two minutes of flushing, and then starts to decay. This observation clearly indicates that most of the lower methylbenzenes are formed by conversion of compounds that are in the gaseous state under standard conditions, and which are therefore not observed in the dissolution experiments. These compounds could be methanol or lower olefins which were adsorbed in the catalyst at the start of the flushing period. The results in Fig. 5 further show that the larger crystals, which have three times more Si than the smaller crystals (see above), contain 2–3 times as many MB molecules throughout the flushing experiment.

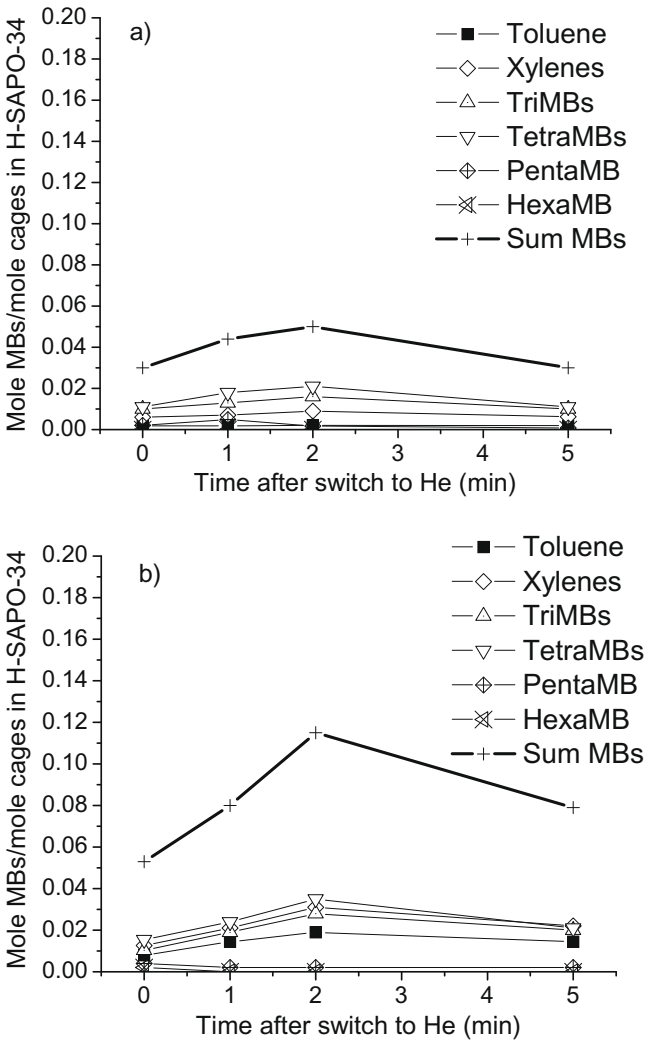

Fig. 5. Retained hydrocarbons detected in H-SAPO-34 (1 μm) (a) and H-SAPO-34 (5 μm) (b) after 3 min of methanol feed at 350 °C, WHSV = 6.2 g/gh and P(MeOH) = 140 hPa, followed by flushing with He for 0–5 min.

3.4. ^{12}C-methanol/^{13}C-methanol switch experiments

The H-SAPO-34 samples were further subjected to ^{12}C-methanol/^{13}C-methanol switch experiments. For H-SAPO-34 (1 μm), ^{12}C-methanol was fed for either 3, 25 or 80 min on stream, and then switched to ^{13}C-methanol under the same conditions. For H-SAPO-34 (5 μm), the isotopic switch was performed after 10 min on stream. In all cases, the ^{13}C content of effluent products and retained hydrocarbons was followed by GC-MS analysis after increasing times on stream, and is shown in Fig. 6–9.

Fig. 6 shows the situation when switching the feed over H-SAPO-34 (1 μm) after 3 min on stream, when the catalyst activity is at its peak, with full methanol conversion. From the gas phase analyses, it is observed that the three main alkene products, C_2–C_4, contain an increasing fraction of ^{13}C, i.e., 76–94% ^{13}C, from 1 to 5 min after switching (Fig. 6a). At each analysis point, the three alkenes contain the same amount of ^{13}C. Propane, which is present in minor amounts (Fig. 2b), also contains an appreciable ^{13}C fraction, ranging from 69% to 88% ^{13}C after 1–5 min of ^{13}C-methanol

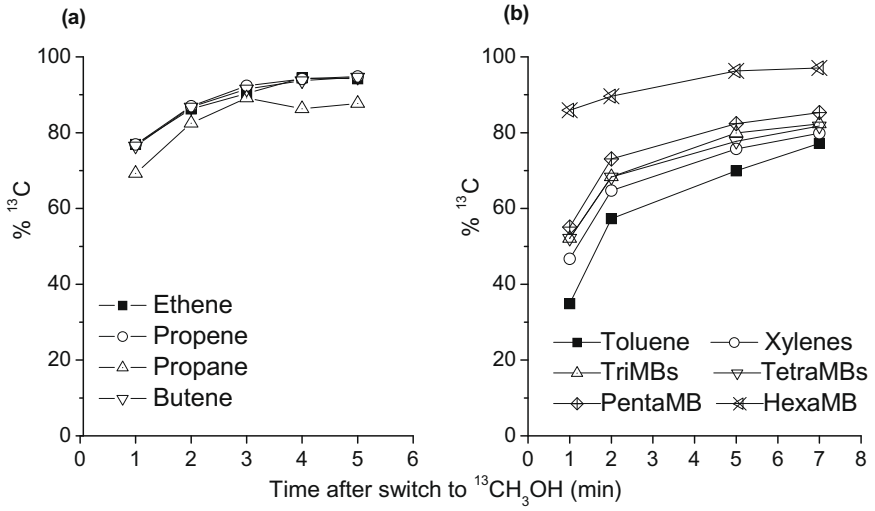

Fig. 6. ^{13}C incorporation into effluent products (a) and retained hydrocarbons (b) in H-SAPO-34 (1 μm) after ^{12}C-methanol was switched to ^{13}C-methanol after 3 min on stream at 350 °C, WHSV = 6.2 g/gh and P(MeOH) = 140 hPa.

feed. However, the ^{13}C content in propane is slightly inferior to that in the C_2–C_4 alkenes at each analysis point. For the retained hydrocarbons, a similar increase in ^{13}C fraction as in the gas phase products is observed with time after switching (Fig. 6b). At each analysis point, hexaMB contains the highest fraction of ^{13}C (86–97%), followed by pentaMB (58–87%), tetraMBs (52–82%), triMBs (52–82%), xylenes (47–80%), and toluene (35–77%). The same order of increasing ^{13}C content with an increasing number of methyl groups in methylbenzene molecules after ^{12}C/^{13}C-methanol switch has been reported previously for H-SAPO-34 and led to the conclusion that hexaMB is the main reaction intermediate in this catalyst [10]. However, opposite to the previous study, the ^{13}C content in hexaMB is in the present case slightly higher than that in the produced alkenes, while in the previous study it was lower in all methylbenzenes compared to the alkenes. This result will be further discussed below. Detailed investigation of the isotopic distribution of each methylbenzene in Fig. 6 showed that 97% of all retained methylbenzene molecules contained at least 1 ^{13}C, 7 min after the switch. This result shows that close to all methylbenzenes retained in the catalyst bed are accessible to the methanol feed after 3 min on stream.

Results obtained when switching from ^{12}C- to ^{13}C-methanol over H-SAPO-34 (1 μm) after 25 min on stream are shown in Fig. 7. At this point, the catalyst still gives close to full methanol conversion, but contains appreciable amounts of coke (see Fig. 2a). Considering first the effluent products (Fig. 7a) the ^{13}C content in the C_2–C_5 alkenes is very similar at each analysis point, and increases from close to 70% to close to 90% ^{13}C during 1–5 min after switching. The only saturated hydrocarbon that is present in appreciable amounts, propane, contains significantly less ^{13}C than the alkenes, i.e., 62–83% ^{13}C during 1–5 min of ^{13}C-methanol feed, with the difference between alkenes and propane being larger than in the experiment mentioned above (Fig. 6a). Considering the retained hydrocarbons in the catalyst (Fig. 7b), the ^{13}C content increases with an increasing number of methyl groups on the benzene ring at each analysis point. Further, the ^{13}C content of all residues increases with an increasing time after switching. The difference in ^{13}C content between the various polyMBs is now more pronounced than in the experiment above (switching after 3 min on stream instead of 25 min on stream). This observation may be exemplified by toluene, in which ^{13}C content increased from 33% to 77% when switching after 3 min on stream, and from 20% to 37% when switching after 25 min on stream. Even hexaMB contains less ^{13}C when switching after 25 min on stream (75–86%) than when switching after 3 min on stream (86–97%). Further, it is interesting to note that all polyMBs now contain less ^{13}C than the alkenes in the effluent at each analysis point after switching. Detailed investigation of the isotopic distribution of each methylbenzene in Fig. 7 showed that 86% of all retained methylbenzene molecules contained at least 1 ^{13}C, 8 min after the switch. This result suggests that although full methanol conversion is observed after 25 min on stream, part of the catalyst crystals are already deactivated, and methylbenzenes retained in the closed parts of those crystals are no longer accessible to the methanol feed, and therefore not participating in alkene formation reactions.

Results obtained when switching from ^{12}C- to ^{13}C-methanol over H-SAPO-34 (1 μm) after 80 min on stream are shown in Fig. 8. At this point, the catalyst approaches complete deactivation (3% conversion, see Fig. 2a). Two changes are apparent compared to the situation at full catalyst activity above: First, there is now a dramatic difference between the ^{13}C content of the alkane and alkenes in the reactor effluent (Fig. 8a); the alkenes having a much higher ^{13}C content (more than 70% ^{13}C after 1 min of ^{13}C-methanol feed) than propane (20% ^{13}C after 1 min of ^{13}C-methanol feed).

The ^{13}C content in the C_2–C_4 alkenes is still similar at each analysis point. Second, among the retained hydrocarbons (Fig. 8b), the ^{13}C content is much lower when switching after 80 min on stream than after 3 or 25 min on stream (compare Figs. 6–8): Among the detected methylbenzenes, pentaMB contains most ^{13}C (8–24%), followed by tetraMBs (2.5–5.6%), triMBs (1.7–2.3%), xylenes (1–2%), and toluene (1.0–1.1%). The amount of hexaMB was low and overlapping with methylnaphthalene signals in the GC-MS, therefore its isotopic composition could not be determined. Among the methylated naphthalene (MN) molecules (not shown), the ^{13}C content never exceeds 5% during 7 min of ^{13}C-methanol feed. A small increase in ^{13}C content is observed for all MBs and MNs from 1 to 7 min of ^{13}C-methanol feed, but the ^{13}C content of all retained molecules apart from pentaMB is still below 6% after 7 min of ^{13}C-methanol feed. Detailed investigation of the isotopic distribution of each methylbenzene in Fig. 8 showed that only 20% of all retained methylbenzene molecules contained at least 1 ^{13}C, 7 min after the switch. Conversely, this result shows that 80% of the retained hydrocarbons in the almost completely deactivated catalyst are no longer accessible to the methanol feed.

The ^{13}C content of effluent products in H-SAPO-34 (5 μm), detected during 1–4 min after switching from ^{12}C- to ^{13}C-methanol,

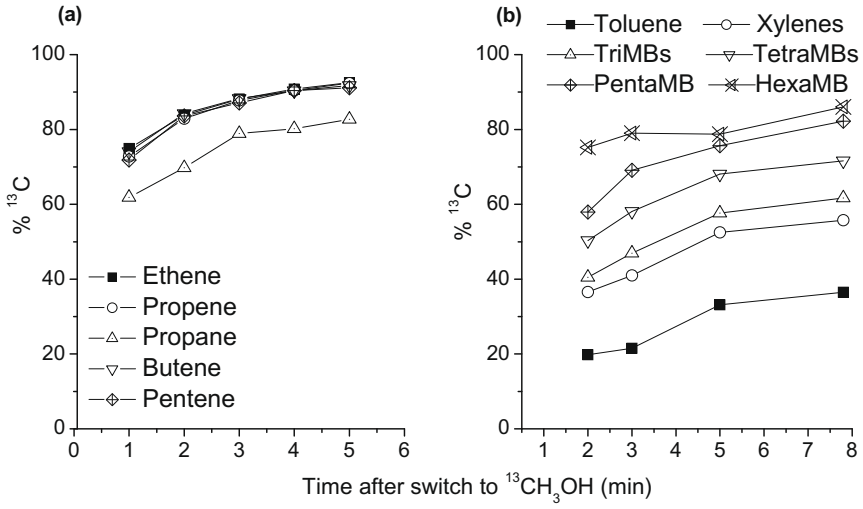

Fig. 7. ^{13}C incorporation into effluent products (a) and retained hydrocarbons (b) in H-SAPO-34 (1 μm) after ^{12}C-methanol was switched to ^{13}C-methanol after 25 min on stream at 350 °C, WHSV = 6.2 g/gh and P(MeOH) = 140 hPa.

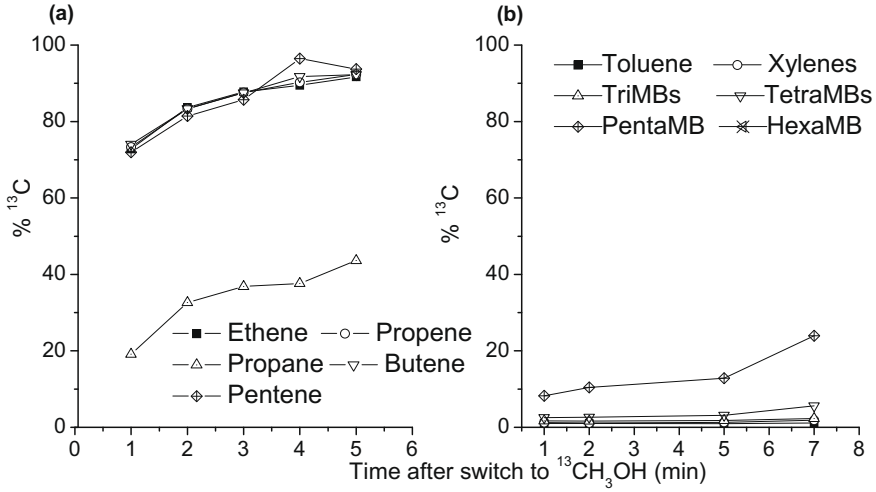

Fig. 8. ^{13}C incorporation into effluent products (a) and retained hydrocarbons (b) in H-SAPO-34 (1 μm) after ^{12}C-methanol was switched to ^{13}C-methanol after 80 min on stream at 350 °C, WHSV = 6.2 g/gh and P(MeOH) = 140 hPa.

as well as retained hydrocarbons analyzed 7 min after switching, is shown in Fig. 9. The switch was performed after 10 min on stream, i.e., when the catalyst approached complete deactivation (5% conversion, see Fig. 2c). The ^{13}C distribution pattern is very similar to that observed for deactivated H-SAPO-34 (1 μm) mentioned above: Among the effluent products, the ^{13}C content of the alkenes (76–96% ^{13}C after 1–4 min of ^{13}C-methanol feed) is much higher than that of propane (1–4% ^{13}C after 1–4 min of ^{13}C-methanol feed) (Fig. 9a). Among the retained hydrocarbons, the ^{13}C content observed 7 min after switching decreases with a decreasing number of methyl groups on the benzene ring, i.e., pentaMB (32% ^{13}C), followed by tetraMBs (6% ^{13}C), triMBs (5% ^{13}C), xylenes (3% ^{13}C), and toluene (2% ^{13}C). Among the methylnaphthalenes (not shown), the ^{13}C content does not exceed 10%. Only 23% of the methylbenzene molecules contained at least 1 ^{13}C 7 min after the switch, showing that 77% of the methylbenzenes are no longer accessible to the methanol feed. Although only one analysis point exists for the retained hydrocarbons in this case, the trend is similar to that observed for the smaller H-SAPO-34 (1 μm) catalyst mentioned above and there is no reason to expect that the evolution with time on stream would be different in the present case than for the smaller catalyst crystals.

4. Discussion

4.1. Reaction selectivity

Under optimized MTO conditions, H-SAPO-34 can produce up to 80% total yield of ethene and propene [45]. The desired propene versus ethene yield depends on the projected market growth rates for each alkene, and recently, propene yield optimization has been emphasized [45]. Several authors reported a change in the ethene-to-propene ratio over H-SAPO-34 with time on stream, favoring ethene production at longer times on stream [33,34]. The same trend is observed in the present work, as evidenced from Fig. 2, and the main aim of this study was to elucidate the reason for this trend, as input to further catalyst optimization. As already described in the Introduction, it is debated whether the observed change is due to transition-state shape selectivity [32,33] or to product shape selectivity [31,34], which is modified by coking.

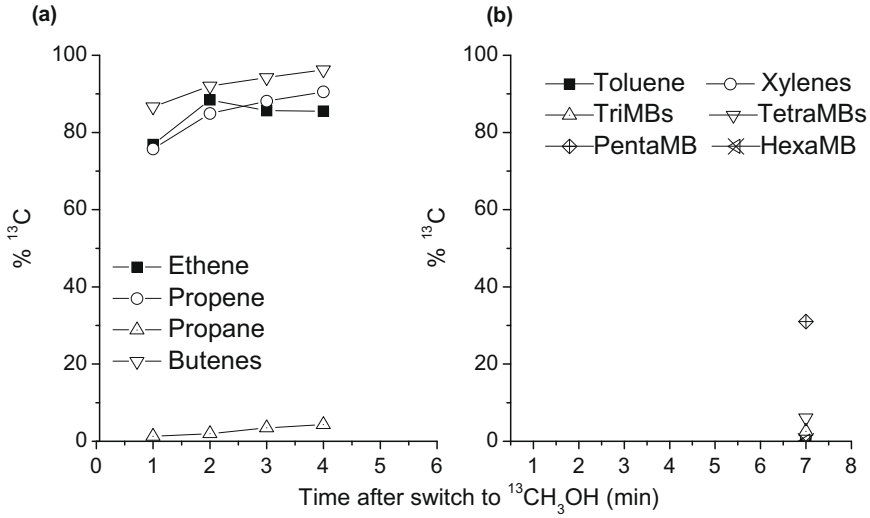

Fig. 9. ^{13}C incorporation into effluent products (a) and retained hydrocarbons (b) in H-SAPO-34 (5 μm) after ^{12}C-methanol was switched to ^{13}C-methanol after 10 min on stream at 350 °C, WHSV = 6.2 g/gh and P(MeOH) = 140 hPa.

From the results reported in Figs. 6–9 mentioned above, catalyst deactivation and its influence on product selectivity may be followed in detail from transient isotopic switch experiments. Concentrating first on the results obtained for the smaller catalyst crystals, H-SAPO-34 (1 μm), it is observed that the incorporation of ^{13}C in effluent products is efficient at all times on stream, leading to more than 70% ^{13}C in all alkene products already 1 min after switching, even for the almost completely deactivated catalyst (Fig. 6–8). The ^{13}C content of all alkenes, 1–5 min after switching, after 3, 25, and 80 min on stream, is plotted together in Supplementary material, Figure S9. The difference is surprisingly small between a fully active and a near completely deactivated sample. Moreover, the ^{13}C content is the same in all alkenes at any time in the experiments. This observation could indicate either that all alkenes are formed by the same mechanism from methylbenzene intermediates in which ^{12}C and ^{13}C are fully equilibrated between ring and methyl groups, or that the alkenes undergo reactions by which they are isotopically equilibrated, after formation, and before diffusing out of the catalyst crystals, or both. Evidence for the first explanation is found by a comparison between the ^{13}C content of the alkene products and the most active methylbenzene intermediate (hexaMB) for the fully active catalyst (switch after 3 min on stream). At this point in time, hexaMB contains similar fractions of ^{13}C to those of the alkenes at any point after the switch. This result is in agreement with those obtained earlier for H-ZSM-5 and H-Beta zeolites [28,29], and is an indication of full equilibration between ring and methyl group carbons in the intermediates.

The ^{13}C content of the only alkane present in significant amounts in the effluent, propane, is lower than that in the alkenes at all times after switching, and the difference increases for more deactivated catalysts. There is no straightforward explanation to this observation, but it could be related to propane being a secondary product from the alkenes, and related to aromatics formation, where a similar, low ^{13}C content is observed for deactivated samples. It could also be related to slow diffusion of propane out of the strongly deactivated catalyst crystals.

Turning to the retained hydrocarbons, the fraction of ^{13}C in the methylbenzene molecules decreases in the order: HexaMB > PentaMB > TetraMBs > TriMBs > Xylenes> Toluene at all points after the ^{12}C-/^{13}C-methanol switch, for active as well as deactivated catalysts (Fig. 6–8). This result clearly indicates that hexaMB is the most active intermediate in the MTO reaction over H-SAPO-34 catalysts, even for severely deactivated catalysts. From this result, we may conclude that the selectivity change observed with time on stream over H-SAPO-34 is not due to transition-state shape selectivity, but must be due to product shape selectivity, even for a severely deactivated catalyst.

Haw et al. reached the opposite conclusion about transition-state selectivity versus product shape selectivity compared to the present study, based on a decreasing number of methyl groups on retained methylbenzenes in the catalyst with time on stream [33]. Our results are in full accordance with their results, i.e., the composition of retained hydrocarbons is shifted toward lighter methylbenzenes with time on stream (see Fig. 3). However, the isotopic switch data clearly demonstrate that most of these light methylbenzenes are not accessible to the methanol feed in deactivated catalysts. This result implies that the lighter methylbenzenes are not involved in the MTO reaction, and are therefore irrelevant for the selectivity issue.

The results obtained over the larger catalyst crystals, H-SAPO-34 (5 μm), are in agreement with those obtained over the smaller crystals: For the severely deactivated catalyst, the ^{13}C fraction in the alkenes in the effluent is high and increases with an increasing time after switching from ^{12}C- to ^{13}C-methanol, while it is much lower for propane (Fig. 9a). The ^{13}C fraction in the retained hydrocarbons is lower than that in the alkenes, and decreases with a decreasing number of methyl groups on the benzene ring (Fig. 9b). These results confirm the conclusion of product shape selectivity drawn for the smaller crystals above, and suggest that this conclusion is generally valid for H-SAPO-34 catalysts.

4.2. Catalyst deactivation

Catalyst deactivation in H-SAPO-34 is generally accompanied by the progressive formation of polyaromatic molecules, which are gradually converted to large coke fragments [11,36]. The results obtained in the present study are no exception to this trend, as can be evidenced from Fig. 2a and c as well as Figs. 3 and 4. However, the combination of following the retained hydrocarbons far beyond complete deactivation of the catalysts (Figs. 3 and 4), the quantification of retained hydrocarbons during flushing experiments (Fig. 5a and b) and isotopic switch experiments performed at increasing times on stream, covering the whole deactivation cycle (Figs. 6–9), reveals interesting, novel information about the deactivation pattern of H-SAPO-34 catalysts.

Turning first to the results shown in Figs. 3 and 4, it is clear that the composition of the retained hydrocarbons is not the same at the time of near complete deactivation for the smaller (Fig. 3, 80 min on stream) and larger (Fig. 4, 15 min on stream) catalyst crystals. At the time of near complete deactivation of the smaller crystals, H-SAPO-34 (1 μm), the main retained hydrocarbons are triMBs, followed by xylenes, methylnaphthalenes, and toluene. The catalyst also contains appreciable amounts of three- and four-ring aromatic compounds (Fig. 3). In the larger crystals, H-SAPO-34 (5 μm), the distribution of retained hydrocarbons is quite different at the time of near complete deactivation (15 μm): The tetraMBs are still the main retained hydrocarbons, followed by xylenes, triMBs, and toluene, quite similar to the situation at close to full activity (5 min on stream). Only a small amount of indenes and naphthalenes are observed after 15 min on stream (Fig. 4). Well beyond complete deactivation, the amount of retained hydrocarbons increases and is shifted to heavier compounds for both catalysts, with methylnaphthalene becoming the most abundantly retained hydrocarbon after the longest time on stream, and three- and four-ring polyaromatics being present in both catalysts (Figs. 3 and 4). Considering the amount of retained hydrocarbons, it increases with time on stream even after complete deactivation of the smaller catalyst crystals (Fig. 3), and it is in particular the amount of toluene, xylenes, triMBs, naphthalenes, and three- and four-ring aromatics which increases. This increase could be either due to methanol entering the crystals and reacting with retained hydrocarbons in the deactivated crystals, or due to reactions between methanol and/or gaseous MTO products that are trapped inside deactivated catalyst crystals. The results presented in Fig. 5a, where the amount of retained hydrocarbons increased by a factor of 2–3 during flushing with He, show that the latter explanation may be valid. Turning to the results in Fig. 8b, they clearly support the hypothesis of reactions between trapped methanol and/or gaseous MTO reaction products as a main source of retained hydrocarbons: When switching from ^{12}C- to ^{13}C-methanol after 80 min on stream, all retained hydrocarbons that increase in abundance contain less than 6% ^{13}C, even 7 min after the switch. Furthermore, the isotopic distribution for these products showed that as much as 93% of toluene, 89% of xylenes, 86% of triMBs, 74% of tetraMBs, and 39% of pentaMB contained only ^{12}C, and no ^{13}C 7 min after the switch. Further evidence of reactions between trapped molecules as a main source of retained hydrocarbons is found from the results obtained over the larger catalyst crystals, H-SAPO-34 (5 μm). When switching from a ^{12}C- to a ^{13}C-methanol feed after 10 min on stream over the same catalyst, the ^{13}C content in the retained hydrocarbons was only 1–6% after an additional 7 min of ^{13}C-methanol feed (Fig. 9), except for pentaMB, which contained 32% ^{13}C and constituted a very minor fraction of the residue (see Fig. 4). These results clearly indicate that the major fraction of aromatic molecules in the strongly deactivated catalyst is formed in parts of catalyst crystals that are not accessible to the methanol feed.

Together, the results obtained in the present study strongly indicate that only a small fraction of the catalyst bed, and even only a small fraction of each catalyst crystal, is active for the MTO reaction at any point in time. Focusing on the smaller crystals, H-SAPO-34 (1 μm), the results in Fig. 5a show that only 3% of the cages in the catalyst bed contained a methylbenzene molecule after 3 min on stream, where full methanol conversion is observed. At this time on stream, isotopic switch experiments showed that ~ all methylbenzene molecules were accessible to the methanol feed, since 97% of those molecules contained at least 1 ^{13}C after the ^{12}C-/^{13}C-methanol switch (see Fig. 6b). After 25 min on stream, the situation has changed: Even though the catalyst still gives full methanol conversion (Fig. 2a), the fraction of methylbenzenes which contain at least 1 ^{13}C, 8 min after the switch, has decreased to 86%. Integration of the methylbenzene signals in Fig. 3 (see Supplementary material, Figure S4) indicates a MB molecule-to-H-SAPO-34 cage ratio of 0.11 at this point, suggesting that only 10% of the H-SAPO-34 cages contained methylbenzenes which could participate in the MTO reaction after 25 min on stream. After 80 min on stream, when the catalyst is almost completely deactivated, only 20% of the MBs contained at least 1 ^{13}C, 7 min after the switch. Integration of the MB amounts indicates a MB molecule-to-H-SAPO-34 cage ratio of 0.22 (see Supplementary material), suggesting that only 4% of the H-SAPO-34 cages contained methylbenzenes which could participate in the MTO reaction at this point. The much lower conversions obtained after 80 min on stream compared to 3 min on stream, in spite of a similar fraction of accessible methylbenzenes, suggests that while methanol diffusion into the crystals is rapid after 3 min on stream, reaction with most of the accessible methylbenzenes is hindered by increased diffusion restrictions after 80 min on stream. Together, these results indicate that a maximum of 10% of the H-SAPO-34 (1 μm) cages in the catalyst bed has contributed to alkene production at any point in time during the test cycle.

The results discussed in the former sections may further explain the discrepancy between the ^{12}C-/^{13}C-methanol switch results obtained in this study and those obtained in a previous study by Arstad and Kolboe, referred to in the Results section above: They performed the isotopic switch after 6 min on stream (at 325 °C), when the catalyst activity was already decreasing [10]. The lower ^{13}C content observed in the polyMBs (even for hexaMB) compared to that in the alkenes in their case probably means that part of their catalyst was already clogged, and not participating in the MTO reaction.

The total coke content of the catalysts during and after testing is much higher than the total weight of retained hydrocarbons at any time on stream for both catalysts. The final coke content of H-SAPO-34 (1 μm) is 16.5 wt% (Fig. 2a), which would correspond to, e.g. one molecule of triMB in each catalyst cage. However, integration of the retained hydrocarbons in Figs. 3 and 4 (see Supplementary material, Figures S4 and S5) shows that the total number of retained methylbenzenes never exceeds 25% of the total number of H-SAPO-34 cages in the catalyst bed. As discussed above, a significant fraction of the coke which is not detectable by the dissolution-extraction method (i.e., retained hydrocarbons) after short times on stream is probably trapped product molecules in the gaseous state, which are oxidized and/or may diffuse out of the catalyst under coke oxidation conditions in the thermogravimetric weight. With time on stream, insoluble coke becomes more abundant, and is observed as insoluble black spots during the dissolution-extraction experiments.

Together, the results discussed in this section suggest that H-SAPO-34 deactivates by clogging of the outermost part of the catalyst crystals by product molecules (aliphatic or aromatic), followed by the formation of polyaromatic molecules from trapped alkenes (and methanol) inside the deactivated crystals. It cannot be deduced from the present study whether clogging takes place at the exterior of the catalyst or in the outermost layer of cages. However, in a very recent publication, Weckhuysen et al. followed large H-SAPO-34 crystals by in situ spectroscopy during the MTO reaction and observed that fluorescent molecules were formed with time on stream inside the crystals, but not on the outer surface of the crystals [46].

5. Conclusion

The results obtained in this study present a new perspective of catalyst deactivation in the MTO reaction over H-SAPO-34 catalysts. Initially, methanol is free to diffuse into the crystals and adsorb at acidic sites. During the induction period, methylbenzene

molecules are formed, mainly in the outer cages of the crystals, and lead to the formation of alkene products, which may diffuse out of the crystals and into the gas phase. However, some products are too bulky to escape through the cage windows, and remain in the cages, where they hinder diffusion of smaller reactant and product molecules, thereby contributing to catalyst deactivation. Increased diffusion hindrance further leads to a shift in product selectivity, in favor of the lighter alkene, ethene. With time on stream, reactant and product molecules which are trapped inside the crystals react further to form polyaromatic compounds. Such compounds had previously been assumed to be responsible for the deactivation of H-SAPO-34 catalysts during the MTO reaction, but our results show that they are mainly formed after deactivation has taken place.

Acknowledgments

The authors thank the Norwegian Research Council for financing this study through Grant No. 174893. B.P.C.H. thanks the European Commission Erasmus program, the Prestige Master Nanomaterials: Chemistry & Physics and K.F. Hein fonds for a mobility grant.

Appendix A. Supplementary data

Supplementary data associated with this article can be found, in the online version, at doi:10.1016/j.jcat.2009.03.009.

References

[1] S. Kvisle, T. Fuglerud, S. Kolboe, U. Olsbye, K.-P. Lillerud, B.V. Vora, Handbook of Heterogeneous Catalysis, second ed., 2008, pp. 2950–2965.
[2] C.D. Chang, A.J. Silvestri, J. Catal. 47 (1977) 249.
[3] M. Stöcker, Micropor. Mesopor. Mater. 29 (1999) 3.
[4] I.M. Dahl, S. Kolboe, Catal. Lett. 20 (1993) 329.
[5] I.M. Dahl, S. Kolboe, J. Catal. 149 (1994) 458.
[6] I.M. Dahl, S. Kolboe, J. Catal. 161 (1996) 304.
[7] P.W. Goguen, T. Xu, D.H. Barich, T.W. Skloss, W. Song, Z. Wang, J.B. Nicholas, J.F. Haw, J. Am. Chem. Soc. 120 (1998) 2650.
[8] Ø. Mikkelsen, P.O. Rønning, S. Kolboe, Micropor. Mesopor. Mater. 40 (2000) 95.
[9] W. Song, J.F. Haw, J.B. Nicholas, C.S. Heneghan, J. Am. Chem. Soc. 122 (2000) 10726.
[10] B. Arstad, S. Kolboe, J. Am. Chem. Soc. 123 (2001) 8137.
[11] B. Arstad, S. Kolboe, Catal. Lett. 71 (2001) 209.
[12] A. Sassi, M.A. Wildman, H.J. Ahn, P. Prasad, J.B. Nicholas, J.F. Haw, J. Phys. Chem. B 106 (2002) 2294.
[13] A. Sassi, M.A. Wildman, J.F. Haw, J. Phys. Chem. B 106 (2002) 8768.
[14] M. Bjørgen, U. Olsbye, S. Kolboe, J. Catal. 215 (2003) 30.
[15] M. Bjørgen, F. Bonino, S. Kolboe, K.-P. Lillerud, A. Zecchina, S. Bordiga, J. Am. Chem. Soc. 125 (2003) 15863.
[16] M. Seiler, W. Wang, A. Buchholz, M. Hunger, Catal. Lett. 88 (2003) 187.
[17] M. Bjørgen, U. Olsbye, S. Svelle, S. Kolboe, Catal. Lett. 93 (2004) 37.
[18] M. Bjørgen, U. Olsbye, D. Petersen, S. Kolboe, J. Catal. 221 (2004) 1.
[19] B. Arstad, J.B. Nicholas, J.F. Haw, J. Am. Chem. Soc. 126 (2004) 2991.
[20] U. Olsbye, M. Bjørgen, S. Svelle, K.-P. Lillerud, S. Kolboe, Catal. Today 106 (2005) 108.
[21] S. Svelle, M. Bjørgen, S. Kolboe, D. Kuck, M. Letzel, U. Olsbye, O. Sekiguchi, E. Uggerud, Catal. Lett. 109 (2006) 25.
[22] W. Wang, Y. Jiang, M. Hunger, Catal. Today 113 (2006) 102.
[23] D.M. McCann, D. Lesthaeghe, P.W. Kletnieks, D.R. Guenther, M.J. Hayman, V. Van Speybroek, M. Waroquier, J.F. Haw, Angew. Chem. Int. Ed. 47 (2008) 5179.
[24] R.F. Sullivan, C.J. Egan, G.E. Langlois, R.P.J. Sieg, Am. Chem. Soc. 83 (1961) 1156.
[25] T. Mole, G. Bett, D. Seddon, J. Catal. 84 (1983) 435.
[26] J.F. Haw, W. Song, D.M. Marcus, J.B. Nicholas, Acc. Chem. Res. 36 (2003) 317.
[27] L.-T. Yuen, S.I. Zones, T.V. Harris, E.J. Gallegos, A. Auroux, Micropor. Mater. 2 (1994) 105.
[28] S. Svelle, U. Olsbye, F. Joensen, M. Bjørgen, J. Phys. Chem. C 111 (2007) 17981.
[29] S. Svelle, F. Joensen, J. Nerlov, U. Olsbye, K.-P. Lillerud, S. Kolboe, M. Bjørgen, J. Am. Chem. Soc. 1238 (2006) 14770.
[30] M. Bjørgen, S. Svelle, F. Joensen, J. Nerlov, S. Kolboe, F. Bonino, L. Palumbo, S. Bordiga, U. Olsbye, J. Catal. 249 (2007) 195.
[31] D. Chen, K. Moljord, T. Fuglerud, A. Holmen, Micropor. Mesopor. Mater. 29 (1999) 191.
[32] I.M. Dahl, R. Wendelbo, A. Andersen, D. Akporiaye, H. Mostad, T. Fuglerud, Micropor. Mesopor. Mater. 29 (1999) 159.
[33] W. Song, J.F. Haw, J. Am. Chem. Soc. 123 (2001) 4749.
[34] P. Barger, M. Guisnet, J.-P. Gilson (Eds.), Zeolites for Cleaner Technologies, Catal. Sci. Series 3, Imperial College Press, Danvers, 2002, pp. 239–260.
[35] W. Song, J.F. Haw, Angew. Chem. Int. Ed. 42 (2003) 892.
[36] H. Fu, W. Song, J.F. Haw, Catal. Lett. 76 (2001) 89.
[37] W. Song, H. Fu, J.F. Haw, J. Phys. Chem. B 105 (2001) 12839.
[38] B.M. Lok, C.A. Messina, R.L Patton, R.T. Gajek, T.R. Cannan, E.M. Flanigan, US Patent 4 440 871 (1984) Example 35.
[39] M. Ito, Y. Shimoyama, Y. Saito, Y. Tsurita, M. Otake, Acta. Cryst. C 41 (1985) 1698.
[40] L. Marchese, A. Frache, E. Gianotti, G. Martra, M. Causà, S. Coluccia, Micropor. Mesopor. Mater. 30 (1999) 145.
[41] D. Chen, K. Moljord, T. Fuglerud, A. Holmen, Micropor. Mesopor. Mater. 29 (1999) 191.
[42] S. Wilson, P. Barger, Micropor. Mesopor. Mater. 29 (1999) 117.
[43] D.M. Marcus, W. Song, L.L. Ng, J.F. Haw, Langmuir 18 (2002) 8386.
[44] F. Bleken, M. Bjørgen, L. Palumbo, S. Bordiga, S. Svelle, K.-P. Lillerud, U. Olsbye, Topics in Catalysis 52 (2009) 218.
[45] J.Q. Chen, A. Bozzano, B. Glover, T. Fuglerud, S. Kvisle, Catal. Today 106 (2005) 103.
[46] D. Mores, E. Stavitski, M.H.F. Kox, J. Kornatowski, U. Olsbye, B.M. Weckhuysen, Chem. Eur. J. 14 (2008) 11320.